Atmospheric Pollution Research 4 (2013) 306-314

Atmospheric Pollution Research

www.atmospolres.com

Integrated modeling of urban–scale pollutant transport: application in a semi–arid urban valley, Northwestern China

Na Liu [1,2], Ye Yu [1], Jianjun He [1,2], Suping Zhao [1,2]

[1] *Key Laboratory of Land Surface Process & Climate Change in Cold & Arid Regions, Cold and Arid Regions Environmental & Engineering Research Institute, Chinese Academy of Sciences, Lanzhou 730000, Gansu, China*
[2] *University of Chinese Academy of Sciences, Beijing 100049, China*

ABSTRACT

Air pollution in urban areas is related not only to emission sources but also to atmospheric dispersion and transport conditions. Knowledge of pollutant transport pathways, potential source regions and their relative contribution to pollution levels in a city is thus very useful for urban planning and development of effective regulatory and mitigation strategies. In this study, the Hybrid Single–Particle Lagrangian Integrated Trajectory (HYSPLIT) model driven by high resolution (1 km×1 km) meteorological fields from the Weather Research & Forecasting (WRF) model was used to identify the relationship between atmospheric transport patterns and daily pollutant concentrations on urban scale, with a case study in Lanzhou–an urban valley in Northwestern China. Trajectories calculated by HYSPLIT model for winter months (December, January and February) of 2002–2008 were analyzed using Ward's hierarchical method to identify dominant transport pathways leading to elevated pollutant concentrations in urban Lanzhou. Potential source locations and their relative contribution to pollution levels were evaluated with the help of potential source contribution function (PSCF) analysis and the concentration–weighted trajectory (CWT) method. The transport pathways from the northeast of the urban center and from the west and the east county were identified as the most important pathways leading to high pollutant concentrations in urban Lanzhou, with potential source areas located in the west and the east to the urban center. The contribution of potential source regions was more than 200 μg m^{-3}, 120 μg m^{-3} and 60–80 μg m^{-3} to the PM_{10}, SO_2 and NO_2 loadings, respectively, which is closely related to emission source characteristics in the study area.

Keywords: *Transport pathway, potential source areas, WRF–HYSPLIT model, cluster analysis*

Corresponding Author:
Ye Yu
☎ : *+86-0-931-4967168*
🖷 : *+86-0-931-4967168*
✉ : *yyu@lzb.ac.cn*

Article History:
Received: 31 January 2013
Revised: 09 May 2013
Accepted: 01 June 2013

doi: 10.5094/APR.2013.034

1. Introduction

Increasing urbanization in the past 200 years over the world has caused many social and environmental problems, one of which attracts particular attention is the urban air pollution (Chan and Yao, 2008; Fang et al., 2009). It has been recognized that the amount of pollutant emitted and the dispersion and transport conditions of the atmosphere are two main factors affecting urban air quality. Many urban areas facing severe air pollution problems are located in valleys. While cities located over plains are very sensitive to regionally transported pollutants, cities in valleys or basins are more sensitive to local pollutants.

Lanzhou, located in the Yellow river valley on the north–eastern verge of the Qinghai–Tibet Plateau, is a typical fast growing city in Northwestern China, with an urban population of about 2.6 million over an area of about 1 700 square kilometers (China's Sixth National Population Census). As the capital of the Gansu province and the geographical center of China, air pollution has been one of the most formidable public health issues in Lanzhou—in the valley the highest concentrations of gaseous and particulate pollutants have been documented in the urban cities in China (Zhang et al., 2001). The valley's trough–shaped topography (Figure 1b) leads to poor dispersion conditions in the city, such as the strong and persisted inversions and the high frequency of calm conditions. The unique topography and poor dispersion conditions, as well as coal burning during heating period, result in very serious pollution in winter (Chen et al., 2010). Actions towards reducing emissions of pollutants have being put into effect, but the level of pollution remains high. Yu et al. (2010) showed that the annual mean mass concentration of PM_{10} in urban Lanzhou has decreased from 236 μg m^{-3} in 2001 to 127 μg m^{-3} in 2007, but still exceeds the national Grade II standard for the annual mean PM_{10} concentration (100 μg m^{-3}) by 27%. Serious air pollution not only affects local or even regional climate and human health, but also limits the development of a city, at the same time, is a challenge to sustain social and economic development. To gain sustained good air quality, it is necessary to better understand the causes and characteristics of air pollution in Lanzhou.

Most of previous studies on air pollution in Lanzhou were focused on the temporal variability of pollutants (Wang et al., 2009; Yu et al., 2010), human health effects (Qian et al., 2004; Zhang et al., 2005), local dispersion characteristics of pollutants (An et al., 2008; Chu et al., 2008) and the impact of dust weather (Wang et al., 2006), with little or no studies on the transport characteristics of air pollutants in Lanzhou. Many studies have shown significant correlation of spatial and temporal variations of pollutants with air mass transport pathways. Air mass trajectories have been frequently used to assess transport pathways of air pollutants (Miller, 1981; Seibert et al., 1994; Wang et al., 2010). Generally, large numbers of trajectories arriving at a specific location are statistically analyzed to identify atmospheric transport patterns (Borge et al., 2007). In recent years, air mass trajectory clustering has been widely applied to identify transport patterns affecting air quality in urban areas (Moody and Galloway, 1988; Harris and Kahl, 1990; Abdalmogith and Harrison, 2005; Coury and Dillner, 2007) with effort to obtain the cause–effect relationship

between atmospheric transport patterns and air quality at a specific location over a relatively long time. Trajectory clustering, potential source contribution function (PSCF) and concentration–weighted trajectory (CWT) methods have been used to gain insights into the source regions and the prevailing transport pathways for airborne particles and gases (Ashbaugh et al., 1985; Stohl and Kromp–Kolb, 1994; Hopke et al, 1995; Stohl, 1996; Hsu et al., 2003; Salvador et al., 2004). One of the widely applied air trajectory model is the Hybrid Single–Particle Langrangian Integrated Trajectory model (HYSPLIT), which was generally used for long–range transport studies (Draxler and Hess, 1997). In most applications, the meteorological input data for trajectory calculations were taken from large–scale models with coarse resolutions, e.g. 1°×1° FNL data from the Air Resource Laboratory (ARL), National Oceanic and Atmospheric Administration (NOAA), which limits the application of trajectory models to relatively large areas with coarse spatial resolutions. In recent years, mesoscale atmospheric models have been increasingly used to capture the complex flow and meteorological conditions essential for pollutant dispersions over complex terrain with high spatial and temporal resolutions (Wang and Ostoja–Starzewski, 2004; Horvath et al., 2012).

In the present study, an integrated WRF–HYSPLIT modeling system was used to understand the spatial distribution characteristics of pollutant transport pathways and to identify the potential source regions that fall in the track of the backward trajectories (transport pathways) during winters of Lanzhou from 2002 to 2008 on a high spatial resolution. Since different transport patterns may play different roles during a certain air pollution episode, clustering results were analyzed to reveal the dominant transport pathways that correspond to elevated pollutant concentrations during air pollution episodes and to explain the causes of air pollution. The results from current research would not only be useful for the development of regulatory and mitigation strategies, but also gain some experience for cities with similar situations in the world.

2. Data and the Study Area

2.1. Overview of the study area

Lanzhou is a typical valley city surrounded by mountains and hills that rise to 200–600 m. The average altitude of the city is about 1 520 m above the sea level (ASL), and the urban area is about 35 km long and 2–8 km wide. There are four districts in urban Lanzhou (Figure 1b), i.e. Chengguan, Qilihe, Xigu, and Anning. The Chengguan district, located in the eastern valley, is the home of government and hosts commercial, cultural, and residential elements. The Xigu district, located in the western valley, is the home of large and heavy industries. The Qilihe and Anning districts, located in the middle and the north–middle portions of the valley, respectively, contain residential areas and small factories. There are also three counties in the east (Yuzhong), the north (Gaolan), and the north–west (Yongdeng) of the city. The special topographic features result in long–lasting inversions and weak surface winds, which inhibit transport and turbulent diffusion of pollutants in the area, especially in winter.

2.2. Data

The PM_{10}, SO_2 and NO_2 concentration data for Lanzhou from 2002 to 2008 were obtained from the local air quality monitoring system maintained by Lanzhou Municipal Environmental Protection Bureau. The outputs from the WRF model were used as meteorological input for HYSPLIT trajectory calculations. The meteorological data were archived every hour. Winter was selected for this study as severe local air pollution in Lanzhou, usually formed under steady weather conditions, occurred most frequently when strong and persisted inversions and high frequency of calm conditions prevail.

3. Methodology

3.1. The WRF model

The Weather Research and Forecasting (WRF) model was used in this study to generate high–resolution meteorological inputs for HYSPLIT. WRF is a non–hydrostatic atmospheric research model capable of resolving the impact of localized topography and urban on synoptic scale systems through nested grids. Several physics options are available in WRF. In this study, the WRF was initialized with the single–moment 6–class microphysics scheme, the Kain–Fritsch cumulus parameterization, the YSU planetary boundary layer scheme, the long–wave Rapid Radiative Transfer Model and the short–wave radiation scheme based on Dudhia (1989). The Noah LSM model was used to explicitly calculate the moisture and heat content of each sub–soil layers.

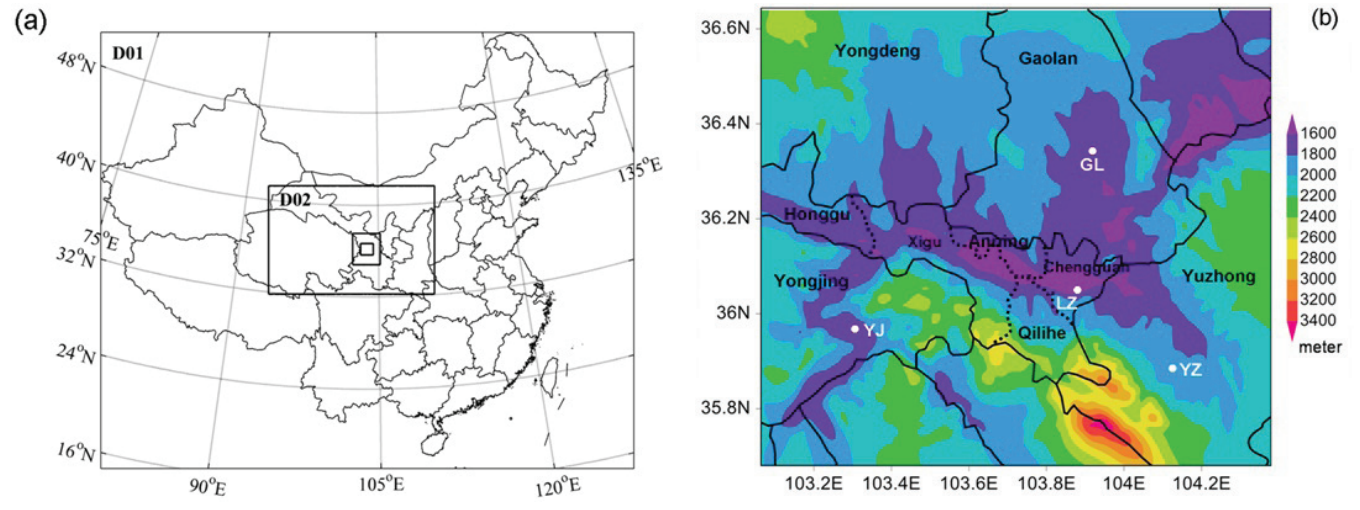

Figure 1. (a) *The four–nested model domains and* ***(b)*** *the topography in the fourth domain covering the urban Lanzhou (i.e. Chengguan, Xigu, Anning and Qilihe districts) and the surrounding counties (Yuzhong, Gaolan and Yongdeng) (m ASL). The white dots represent the four observation sites of the China Meteorological Administration (CMA).*

WRF was configured to have four nested domains at 27, 9, 3, and 1 km resolution with grid cells of 187×153, 174×114, 87×99, and 120×108 in the east–west and the north–south directions for the four domains, respectively (Figure 1a). Vertically there are 36 levels extending from the surface to 50 hpa. The first model level is about 11 m AGL and 12 levels were placed below 1 km for better representation of the atmospheric boundary layer. The National Centers for Environmental Prediction Final Analyses (NCEP FNL) data available at 1°×1° in longitude and latitude every six hours were used as the initial and boundary conditions for WRF simulations. The model was integrated continuously for several 7 day segments and the first 24 h simulations for each integration segment were treated as warm–up period following Otte (2008a; 2008b) and were not used as input for HYSPLIT.

The WRF–modeled 2 m temperature, 10 m wind speed and wind direction were evaluated by comparing with the hourly weather observations from 4 land surface stations (see Figure 1b for the locations) archived at the MICAPS (http://www.cma.gov.cn/en/Special/2012Special/20120504/). Several standard statistical measures were employed for the evaluation (see the Supporting Material, SM, Tables S1 and S2). The results indicate that the model performed well for the study area, with comparable model performance as in other complex terrain areas (e.g. Jimenez et al., 2005; Papalexiou and Moussiopoulos, 2006).

3.2. HYSPLIT trajectory calculation and clustering analysis

HYSPLIT model is a system for computing air mass trajectories and complex dispersion and depositions. It was driven by the WRF simulated high–resolution atmospheric fields to produce backward trajectories of parcels originating from the eastern central urban of Lanzhou (Lat: 36.05°N, Lon: 103.85°E). The backward trajectories provide Lagrangian path of air parcels in the chosen time scale, which could be used to identify the potential source regions and transport pathways of pollutants. Three–dimensional 6 h backward trajectories arriving at the receptor site 100 m above ground level (AGL) were calculated every 6 hour (00, 06, 12, 18 UTC, i.e. 08, 14, 20, 02 Beijing Time) using HYSPLIT–4.9 (Draxler and Hess, 1998) and the meteorological fields from the 1 km resolution WRF domain for winters of 2002–2008. In order to examine the possible effect of regional transport processes, three–dimensional 36 h backward trajectories arriving at the receptor site 100 m above ground level (AGL) were also calculated using the meteorological fields from the larger model domain, i.e. the 9 km resolution WRF domain. Different arrival heights (100, 500, 1 000 m AGL) of backward trajectories were tested and results indicate that the transport pathways are not very sensitive to the selected heights within the studied area.

The final outputs from the WRF–HYSPLIT modeling system were hourly backward trajectory endpoints indicating the geographical location and the height of air parcels. Trajectories were then assigned to distinct clusters according to their moving speed and direction using Ward's hierarchical method based on the Euclidean distance between all pairs of trajectories (Sirois and Bottenheim, 1995). For hierarchical clustering algorithm, the results may change with the number of clusters. In this study, the final number of clusters was determined based on the variation of total spatial variance (TSV) with cluster numbers (see the SM for details). Major transport pathways leading to the elevated pollutant concentrations in winter were identified by combining trajectories with the daily pollutant concentrations.

3.3. Potential source contribution function (PSCF)

The potential source contribution function (PSCF) analysis, combining estimates of the motion of air backward in time with concentrations measured at a receptor site, has been frequently used to identify the probable locations of emission sources that affect pollutant loadings at the receptor site (Hsu et al., 2003). The PSCF values for grid cells in the study domain were calculated by counting the trajectory segment endpoints terminating within each cell, i.e. including trajectories not only ending at the cell but also crossing the cell. By defining the number of endpoints that fall in the ij^{th} cell as n_{ij} and the number of endpoints that corresponds to pollutant concentrations above an arbitrarily set criterion when arriving at the receptor site in the same grid cell as m_{ij}, the PSCF value for the ij^{th} cell is defined as (Ashbaugh et al., 1985):

$$PSCF_{ij} = m_{ij} / n_{ij} \tag{1}$$

The PSCF value represents a conditional probability describing the potential contribution of a grid cell to the high pollutant loadings at the receptor site. Cells with high PSCF values indicate areas of high potential contributions to the pollutant concentration at the receptor site, and the trajectories passing these cells are the major transport pathways leading to the high pollutant loadings at the receptor site. In this study, the mean concentration of pollutants in the seven winters was used as the criterion as in many previous studies (Hsu et al., 2003). For the three pollutants, i.e. PM_{10}, SO_2 and NO_2, the criterions are 197 μg m^{-3}, 103 μg m^{-3} and 66 μg m^{-3}, respectively. To reduce the uncertainty of PSCF resulted from small n_{ij}, an arbitrary weight function W_{ij} proposed by Zeng and Hopke (1989) is multiplied by the PSCF value to better reflect the uncertainty in the values for cells with small n_{ij}. The weight function W_{ij} is defined as:

$$W_{ij} = \begin{cases} 1.00 & n_{ij} > 3 \cdot Avg \\ 0.70 & Avg < n_{ij} \le 3 \cdot Avg \\ 0.42 & 0.5 \cdot Avg < n_{ij} \le Avg \\ 0.17 & 0 < n_{ij} \le 0.5 \cdot Avg \end{cases} \tag{2}$$

where *Avg* is the average number of endpoints in each cell. The weight function reduced the PSCF value when the total number of endpoints in a particular cell was less than about three times the average value of the endpoints per cell (Polissar et al., 2001). Results from PSCF using the 75^{th} percentile of all samples as the criterion were also calculated considering the measurement uncertainty which may change a sample's classification as less than or greater than the criterion.

3.4. Concentration–weighted trajectory (CWT) method

One limitation of the PSCF method is that grid cells may have the same PSCF values when pollutant concentrations at the receptor site are only slightly or extremely higher than the criterions. The PSCF value only gives the spatial distribution of potential source regions without information on the relative significance of different potential source regions. To compensate the limitation, a concentration–weighted trajectory (CWT) method developed by Hsu et al. (2003) was used to calculate the trajectory weighted concentration. In the CWT method, each grid cell is assigned a weighted concentration by averaging the sample pollutant concentrations that have associated trajectories crossing the grid cell as follows:

$$C_{ij} = \frac{1}{\sum_{l=1}^{M} \tau_{ijl}} \sum_{l=1}^{M} C_l \tau_{ijl} \tag{3}$$

where C_{ij} is the average weighted concentration in the ij^{th} cell, l is the index of the trajectory, C_l is the pollutant concentration measured on the arrival of trajectory l, M is the total number of trajectories, and τ_{ijl} is the time spent in the ij^{th} cell by trajectory l. Equation (2) was also applied to the CWT calculation to reduce the uncertainties when n_{ij} is small. A high C_{ij} value implies that air

parcels traveling over the ij^{th} cell would be associated with high pollutant concentration at the receptor site.

4. Results and Discussion

4.1. Pollution characteristics

PM_{10}, SO_2 and NO_2 concentrations in winters of Lanzhou from 2002 to 2008 are shown in Figure 2. The daily average PM_{10}, SO_2 and NO_2 concentrations for the seven winters were 197 μg m^{-3}, 103 μg m^{-3} and 66 μg m^{-3}, respectively, and there were 228 days, 205 days and 244 days with higher than average concentrations for PM_{10}, SO_2 and NO_2, respectively. The average PM_{10} concentration was much higher than the national Grade II standard for daily mean PM_{10} concentration of 150 μg m^{-3} (GB3095–1996), while the averages of the other two pollutants were less than the national Grade II standard (150 μg m^{-3} for SO_2 and 120 μg m^{-3} for NO_2). However, the PM_{10}, SO_2 and NO_2 concentrations exceeded the Grade II standard by 59.4%, 15.5% and 10.1%, respectively, in the seven winters. In addition, there were 25 days (accounted for 4.4% of the total days in the seven winters) when the national Grade V PM_{10} standard of 420 μg m^{-3} were exceeded. Although the primary pollutant is PM_{10} in Lanzhou, the occurrence of SO_2 as the primary pollutant still exists, and there have been days with NO_2 as the primary pollutant in recent years with the increasing numbers of motor vehicles (Zhang et al., 2010), indicating the shift of pollution from "soot–dominated pollution" to "hybrid vehicle exhaust and soot dominated pollution".

4.2. Association of pollutant concentrations with transport pathways

In winter, air pollution is mainly affected by local pollution sources in Lanzhou, so we firstly focused on the area covered by the WRF 1 km resolution domain. The six clusters (transport pathways) obtained by the clustering algorithm and all the 6 h backward trajectories used for the clustering analysis are shown in Figure 3. The transport routes and the direction of trajectories indicate the geographical areas traveled by air masses before their arrival at the receptor site. The length of the cluster–mean trajectories indicates the transport speed of air masses. The longer is the cluster–mean trajectory, the faster is the air mass. It is seen from Figure 3 that the air masses had paths distributed in the west, the north and the southeast. From the length of the trajectories, it is seen that trajectories from the directions of northeast (cluster 4), north (cluster 3), southeast (cluster 6), and west (cluster 2) is longer and moved faster than those in other directions, while trajectories in clusters 1 and 5 were shorter and moved much slower than trajectories in other clusters.

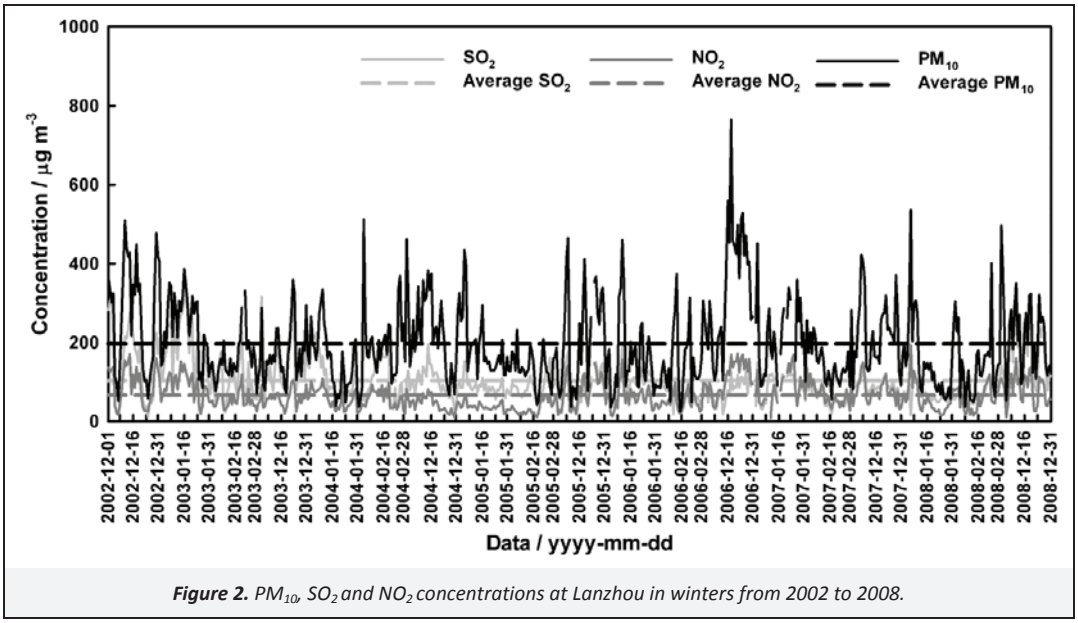

Figure 2. *PM_{10}, SO_2 and NO_2 concentrations at Lanzhou in winters from 2002 to 2008.*

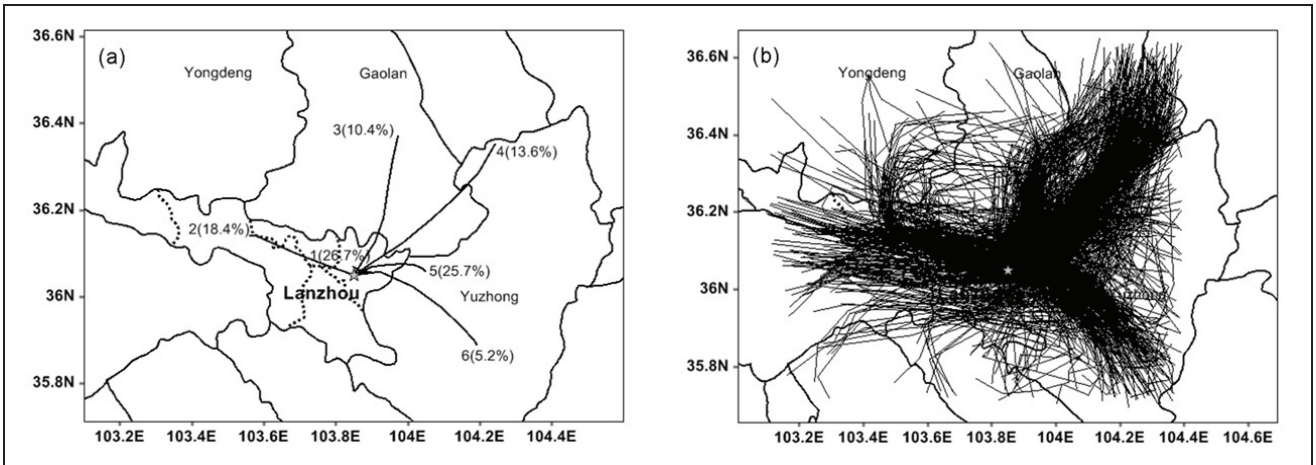

Figure 3. (a) *Six cluster–mean backward trajectories (numbers in brackets indicate the percentage of trajectories allocated to a cluster) and* ***(b)*** *all trajectories. The pentagram in the graph represents the starting point of trajectories or the receptor site used in the study.*

All the backward trajectories are divided into two groups, i.e. the polluted and the clean trajectories, according to the sample pollutant concentrations when they arrived at the receptor site. The polluted trajectories are defined as those with pollutant concentrations higher than the winter averages, i.e. 197 μg m^{-3}, 103 μg m^{-3} and 66 μg m^{-3} for PM_{10}, SO_2 and NO_2, respectively. The number and percentage of polluted trajectories of each cluster are summarized in Table 1, and the corresponding mean concentrations of PM_{10}, SO_2 and NO_2 when the transport pathway arrived at the receptor site are calculated and shown in Table 2.

The average PM_{10}, SO_2 and NO_2 concentrations for clusters 2, 5 and 6 exceeded the winter averages of 197 μg m^{-3}, 103 μg m^{-3} and 66 μg m^{-3} for PM_{10}, SO_2 and NO_2, respectively (see Table 2), with 35%–50% of trajectories being polluted ones (see Table 1), which indicates that the air masses associated with these clusters tend to carry more pollutants and lead to high PM_{10}, SO_2 and NO_2 concentrations at the receptor site. The average concentrations of PM_{10} and NO_2 for cluster 1 exceeded the winter averages of 197 μg m^{-3} and 66 μg m^{-3}, respectively, with more than 40% of trajectories being polluted ones, indicating air masses associated with this cluster would lead to high PM_{10} and NO_2 events in Lanzhou during winter. The average PM_{10} and NO_2 concentrations for clusters 3 and 4 and the average SO_2 concentrations for clusters 1 and 4 were less than the winter averages of the three pollutants, respectively. The above analysis indicates that the pathway from the north is relatively cleaner than that from other directions.

Of all the 1 652 backward trajectories, 25.7% were allocated to cluster 5, of which 39.4%–47.6% were polluted. Cluster 5 represents the second polluted transport pathway for NO_2 and SO_2 and the third polluted transport pathway for PM_{10}, respectively. The air masses associated with cluster 5 originated from the west boundary of the Yuzhong county, where Yuzhong Iron and Steel corporation is located. Cluster 1 had the most trajectories (26.7% of all the trajectories) among the six clusters, of which 35.1%–44.0% were polluted ones, indicating that it is an important transport pathway that may cause high pollutant concentrations at the receptor site. Clusters 1 and 5 represent the most important transport pathways among all the six clusters. It should be noted that the trajectories in cluster 1 is the shortest among all the six clusters, indicating the accumulation of pollutants. Cluster 6 represents one of the most polluted transport pathways with the highest PM_{10} concentrations among the six clusters, but its frequency of occurrence is less than one fifth of clusters 1 and 5. Although there are 43% polluted trajectories for PM_{10} in cluster 6, the small number of trajectories indicates that it is not an important transport pathway that would lead to elevated pollutant concentrations at the receptor site in winter. However, the polluted trajectories in cluster 6 had the highest concentrations for all the three pollutants, indicating that air masses associated with cluster 6 have potential to cause pollution episode with very high pollutant concentrations at the receptor site. The west pathway (cluster 2) has a trajectory membership of about 18.4%, with nearly 50% polluted trajectories for NO_2 and more than 40% polluted trajectories for SO_2 and PM_{10}. The high percentage of polluted trajectories for NO_2 and SO_2 in cluster 2 is related to its origin in the Xigu district where clusters of large industrial facilities with high NO_X and SO_2 emissions are located (see Figure 6d and Table S3 in the SM). Although the pollutant concentrations for polluted trajectories in cluster 2 were relatively low among the six clusters, the pathway represented by cluster 2 was a relatively important pathway that could lead to high pollutant loadings at the receptor site. The northeast pathway (cluster 4) originated from the far north of the Yuzhong county and passed through the Gaolan county, with a trajectory membership of about 13.6% and the lowest pollutant levels at the receptor site, is the cleanest pathway among the six clusters. The north pathway (cluster 3), with a trajectory membership of 10.4% and about 40% polluted trajectories, has the second lowest PM_{10} and NO_2 concentrations among the six clusters, but a relatively high SO_2 concentrations, which is related to the clusters of heating stations in the Chengguan district on its pathway. From the above analyses, it is inferred that clusters 1 and 5 are important transport pathways in the studied domain that could cause high pollutant concentrations at the receptor site, cluster 6 from Yuzhong county is an important transport pathway that may cause episode with very high pollutant concentrations at the receptor site, while cluster 2 from the Xigu district may cause medium pollution events.

It is seen from Table 1 that the percentage of polluted trajectories in each cluster is different for different pollutants. For PM_{10}, cluster 5 has the highest percentage of polluted trajectories, while for the two gaseous pollutants, i.e. SO_2 and NO_2, cluster 2 has the highest percentage of polluted trajectories, which is consistent with the source characteristics along their pathways (see Figure 6d).

Table 1. *Frequency of polluted trajectories corresponding to each cluster*

Cluster	PM_{10} polluted trajectories		SO_2 polluted trajectories		NO_2 polluted trajectories	
	Number	Percent of total	Number	Percent of total	Number	Percent of total
1	180	40.8%	155	35.1%	194	44.0%
2	129	42.4%	141	46.4%	151	49.7%
3	67	39.0%	67	39.0%	75	43.6%
4	83	36.9%	69	30.7%	86	38.2%
5	192	45.3%	167	39.4%	202	47.6%
6	37	43.0%	30	34.9%	34	39.5%

Table 2 *The concentration of PM_{10}, SO_2 and NO_2 associated with all trajectories and polluted trajectories in each cluster*

Cluster	Mean concentrations for all trajectories (μg m^{-3})			Mean concentrations for polluted trajectories (μg m^{-3})		
	PM_{10}	SO_2	NO_2	PM_{10}	SO_2	NO_2
1	201.09±116.15	101.04±59.58	67.45±37.29	313.76±94.43	163.30±55.81	101.38±28.92
2	210.41±104.03	112.26±56.66	73.23±34.70	302.95±88.77	157.59±49.20	99.83±27.92
3	193.24±104.43	106.51±64.17	65.57±37.54	296.66±81.14	167.84±59.33	99.41±29.50
4	180.96±111.29	93.51±52.37	59.68±35.18	292.70±102.89	153.38±51.10	96.58±26.32
5	204.99±106.74	109.86±62.76	68.34±37.93	298.70±81.28	168.96±58.42	100.64±27.95
6	222.69±139.65	105.50±58.87	67.21±37.47	351.24±118.63	169.67±54.83	105.41±28.02

4.3. Potential source regions and their relative contribution

The distribution of PSCF in Lanzhou for winters of 2002–2008 is shown in Figure 4. In the map of PSCF, cells with high PSCF values appeared mainly in Yuzhong County and the Xigu industrial area, that is, the potential source areas most likely leading to above average pollutant concentrations at the receptor site in wintertime were located in the east and the west of the receptor site. Air masses from the potential source areas traveled mainly along the pathways represented by clusters 2, 5 and 6 to the receptor site. The effect of potential source areas are different on PM_{10}, SO_2 and NO_2 concentrations (compare Figure 4a, 4b and 4c). The effect of potential source areas on PM_{10} concentrations is higher in Yuzhong county, while that on SO_2 and NO_2 is higher in the Xigu industrial area.

PSCF modeling divides trajectories between clean and polluted ones based on the winter average pollutant concentrations; small variations in pollutant concentrations might change a trajectory's classification. In order to verify the source regions identified above, PSCF results calculated using the 75th percentile of all the samples as the criterion are shown in Figure 5. The use of a higher concentration as the criteria makes it possible to distinguish between strong and weak sources. Figure 5 shows that the highest PSCF values are from the Xigu industrial district in the west and the industrial areas in the Yuzhong county, which is consistent with the identified source regions in Figure 4.

Figure 6 shows the distribution of weighted trajectory concentrations which gives information on the relative significance of potential source areas to pollutant loadings at the receptor site. The potential source areas represented by high CWT values include Yuzhong County and the Xigu industrial area, respectively. The contribution of these potential source regions to PM_{10} loadings at the receptor site exceeded 200 μg m^{-3}, while that to SO_2 concentrations was more than 120 μg m^{-3}, with most of the cells having high CWT values located in the east of the receptor site. Compared with SO_2, the contribution of potential source areas to NO_2 concentrations was relatively low with CWT values being about 60–80 μg m^{-3} in the Yuzhong county, and slightly higher in the Xigu industrial area. The above results are consistent with the trajectory analysis in Section 4.2 and the PSCF analysis.

There may be regional sources that also contribute to the pollution levels in urban Lanzhou. The PSCF and CWT calculated using the 9 km resolution WRF outputs for a larger domain (see the SM, Figures S2 and S3) confirm the importance of local sources in the studied area and show the advantage of using integrated high–resolution modeling system for urban–scale applications.

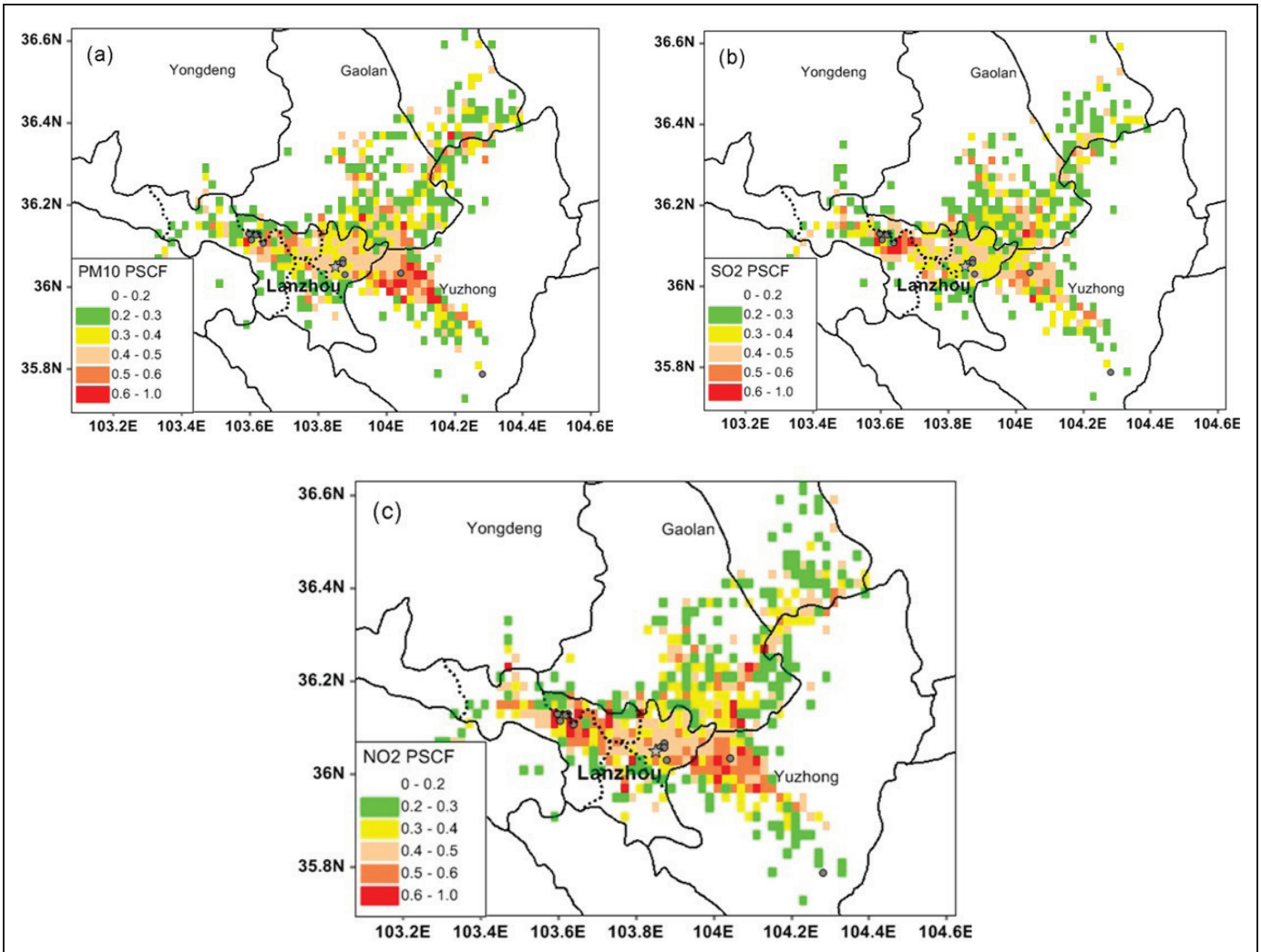

Figure 4. *Potential source contribution function (PSCF) maps for* ***(a)*** *PM_{10},* ***(b)*** *SO_2 and* ***(c)*** *NO_2 in winters during 2002–2008. Darker colors indicate high potential source areas. The dots represent the location of main local emission sources (see Table S3 in the SM for detailed information).*

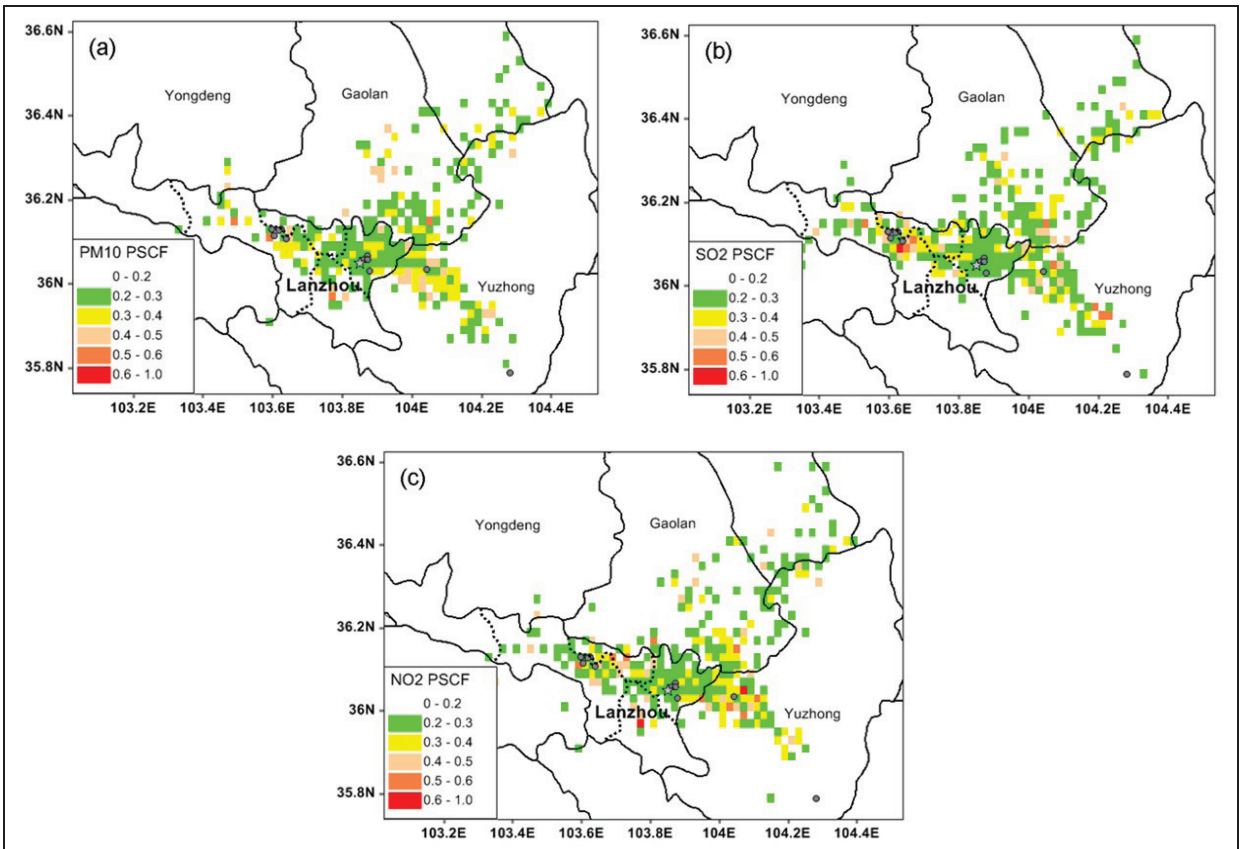

Figure 5. *Same as Figure 4 but for PSCF calculated using the 75th percentile of all the samples as the criterion.*

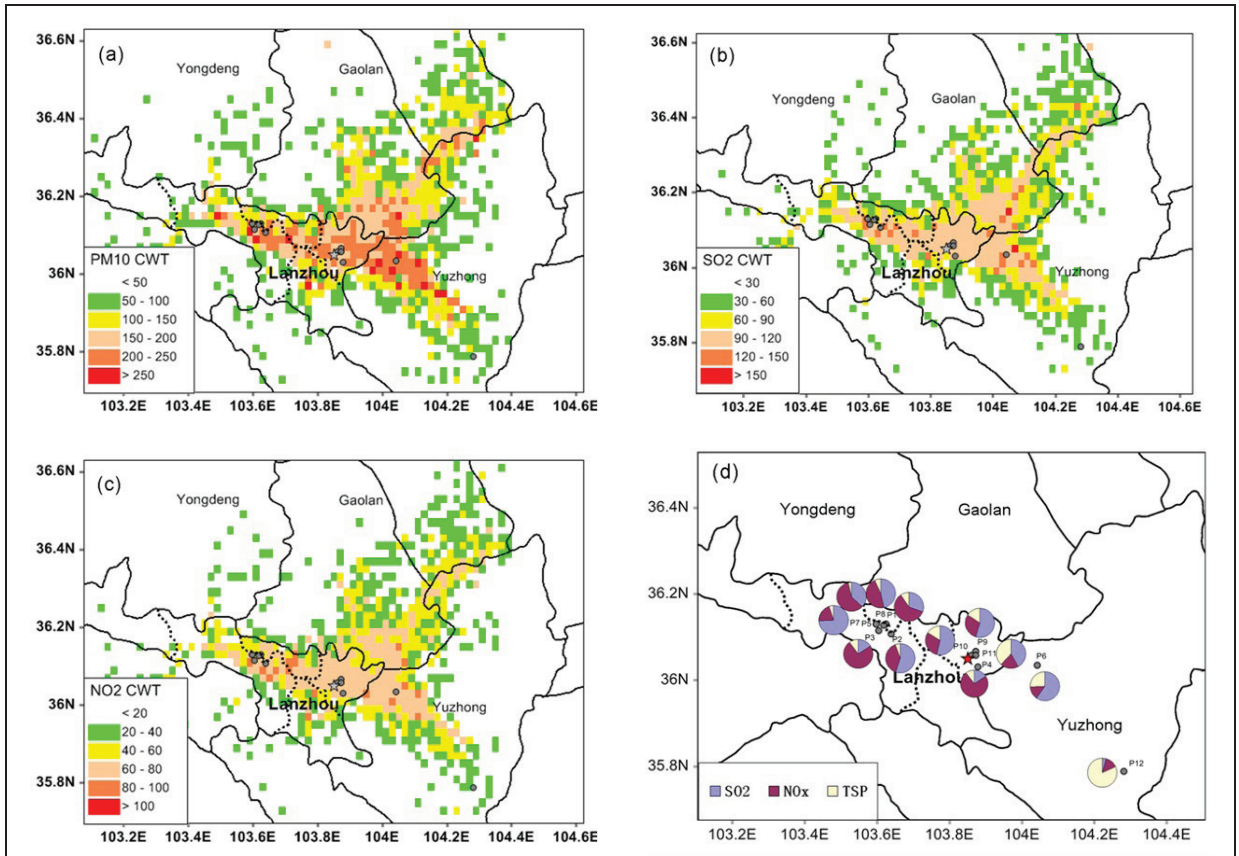

Figure 6. *Concentration–weighted trajectory (CWT) method analysis maps for* ***(a)*** *PM_{10},* ***(b)*** *SO_2,* ***(c)*** *NO_2 and* ***(d)*** *the share of different pollutants in the total emitted pollutants from the main industrial sources listed in Table S3 (see the SM). Darker colors in* ***(a)–(c)*** *indicate greater influence.*

5. Conclusion

The atmospheric transport pathways, potential source areas and their relative contribution to pollutant (PM_{10}, SO_2 and NO_2) loadings in central urban Lanzhou during wintertime were identified by trajectory clustering techniques, potential source contribution function (PSCF) analysis, and concentration–weighted trajectory (CWT) method using the integrated WRF–HYSPLIT model. Results revealed two major transport pathways for the studied domain, including one urban transport pathway (cluster 1 from Chengguan district) and one county transport pathways (cluster 5 from Yuzhong). The county transport pathway, with high frequency of occurrence and high percentage of polluted trajectories, is identified as the most important transport pathway causing high pollutant concentrations at the receptor site, and the urban pathway is the second important transport pathway. While the transport pathway from Gaolan county (clusters 3 and 4) was relatively clean, the long transport pathways from Xigu district (cluster 2) and Yuzhong county (cluster 6) are two pathways that could also cause elevated pollutant concentrations at the receptor site. Two main potential source areas, i.e. the Yuzhong county and the Xigu industrial area were identified using PSCF and CWT. Although the potential source areas are similar for the three pollutants, i.e. PM_{10}, SO_2 and NO_2, their relative importance in causing high pollutant loadings are different.

Results from our study indicate the benefit of using meteorological data with 1 km×1 km resolution from the WRF model as input to the HYSPLIT trajectory model for urban scale pollutant transport studies. The most important transport pathways arriving at the receptor site were identified and the potential source areas and their relative contribution to pollutant concentrations were defined on urban scale. Supplemented with long–term monitoring data with high temporal resolution, e.g. 1 hr, the WRF–HYSPLIT integrated modeling approach could be used for identifying episodic events. Results from this study are not only helpful in guiding the local government for regulating major pollution sources and optimize urban planning, but also gain some experience for cities with similar situations in the world.

Acknowledgements

This research was funded by the Chinese Academy of Sciences through the '100 Talent Project' (No.29 O827631) and the Lanzhou city Science and Technology Plan (No. 2009KJLQ).

Supporting Material Available

Performance statistics of modeled 2–m temperature, 10–m wind speed and wind direction for winters of 2002–2008 at four meteorological stations (Table S1), Definition of Statistical metrics (Table S2), List of main local pollution sources, their locations, and annual emission values of SO_2, NO_X and TSP in tons (Table S3), The methodology employed to select the number of clusters, Backward–trajectory clustering plots (Figure S1), Potential source contribution function (PSCF) maps for (a) PM_{10}, (b) SO_2 and (c) NO_2 in winters during 2002–2008 for the 9–km resolution WRF domain (Figure S2), Concentration–weighted trajectory (CWT) method analysis maps for (a) PM_{10}, (b) SO_2 and (c) NO_2 for the 9–km resolution WRF domain (Figure S3). This information is available free of charge via Internet at http://www.atmospolres.com.

References

Abdalmogith, S.S., Harrison, R.M., 2005. The use of trajectory cluster analysis to examine the long–range transport of secondary inorganic aerosol in the UK. *Atmospheric Environment* 39, 6686–6695.

An, X.Q., Ma, A.Q., Liu, D.B., 2008. A GIS–based study for optimizing the total emission control strategy in Lanzhou City. *Environmental Modeling & Assessment* 13, 491–501.

Ashbaugh, L.L., Malm, W.C., Sadeh, W.Z., 1985. A residence time probability analysis of sulfur concentrations at Grand Canyon National Park. *Atmospheric Environment* 19, 1263–1270.

Borge, R., Lumbreras, J., Vardoulakis, S., Kassomenos, P., Rodriguez, E., 2007. Analysis of long–range transport influences on urban PM_{10} using two–stage atmospheric trajectory clusters. *Atmospheric Environment* 41, 4434–4450.

Chan, C.K., Yao, X., 2008. Air pollution in mega cities in China. *Atmospheric Environment* 42, 1–42.

Chen, L.H, Yu, Y., Chen, J.B., Li, W.Y., Li, J.L., 2010. Characteristics of main air pollution in Lanzhou during 2001–2007. *Plateau Meteorology* 29, 1672–1633.

Chu, P.C., Chen, Y.C., Lu, S.H., 2008. Atmospheric effects on winter SO_2 pollution in Lanzhou, China. *Atmospheric Research* 89, 365–373.

Coury, C., Dillner, A.M., 2007. Trends and sources of particulate matter in the superstition wilderness using air trajectory and aerosol cluster analysis. *Atmospheric Environment* 41, 9309–9323.

Draxler, R.R., Hess, G.D., 1998. An overview of the HYSPLIT_4 modelling system for trajectories, dispersion and deposition. *Australian Meteorological Magazine* 47, 295–308.

Draxler, R.R., Hess, G.D., 1997. Description of the HYSPLIT_4 Modelling System, NOAA Technical Memorandum ERL ARL–224, Silver Spring, Maryland, 24 pages.

Dudhia, J., 1989. Numerical study of convection observed during the Winter Monsoon Experiment using a mesoscale two–dimensional model. *Journal of the Atmospheric Sciences* 46, 3077–3107.

Fang, M., Chan, C.K., Yao, X.M., 2009. Managing air quality in a rapidly developing nation: China. *Atmospheric Environment* 43, 79–86.

Harris, J.M., Kahl, J.D., 1990. A descriptive atmospheric transport climatology for the Mauna Loa Observatory, using clustered trajectories. *Journal of Geophysical Research–Atmospheres* 95, 13651–13667.

Hopke, P.K., Barrie, L.A., Li, S.M., Cheng, M.D., Li, C., Xie, Y., 1995. Possible sources and preferred pathways for biogenic and non–sea–salt sulfur for the high arctic. *Journal of Geophysical Research–Atmospheres* 100, 16595–16603.

Horvath, K., Koracin, D., Vellore, R., Jiang, J.H., Belu, R., 2012. Sub–kilometer dynamical downscaling of near–surface winds in complex terrain using WRF and MM5 mesoscale models. *Journal of Geophysical Research–Atmospheres* 117, art. no. D11111.

Hsu, Y.K., Holsen, T.M., Hopke, P.K., 2003. Comparison of hybrid receptor models to locate PCB sources in Chicago. *Atmospheric Environment* 37, 545–562.

Jimenez, P., Jorba, O., Parra, R., Baldasano, J.M., 2005. Influence of high–model grid resolution on photochemical modelling in very complex terrains. *International Journal of Environment and Pollution* 24, 180–200.

Miller, J.M., 1981. A five–year climatology of back trajectories from the Mauna Loa Observatory, Hawaii. *Atmospheric Environment* 15, 1553–1558.

Moody, J.L., Galloway, J.N., 1988. Quantifying the relationship between atmospheric transport and the chemical composition of precipitation on Bermuda. *Tellus* 40B, 463–479.

Otte, T.L., 2008a. The impact of nudging in the meteorological model for retrospective air quality simulations. Part I: evaluation against national observation networks. *Journal of Applied Meteorology and Climatology* 47, 1853–1867.

Otte, T.L., 2008b. The impact of nudging in the meteorological model for retrospective air quality simulations. Part II: evaluating collocated meteorological and air quality observations. *Journal of Applied Meteorology and Climatology* 47, 1868–1887.

Papalexiou, S., Moussiopoulos, N., 2006. Wind flow and photochemical air pollution in Thessaloniki, Greece. Part II: statistical evaluation of

European Zooming Model's simulation results. *Environmental Modelling & Software* 21, 1752–1758.

Polissar, A.V., Hopke, P.K., Harris, J.M., 2001. Source regions for atmospheric aerosol measured at Barrow, Alaska. *Environmental Science & Technology* 35, 4214–4226.

Qian, Z.M., Chapman, R.S., Hu, W., Wei, F.S., Korn, L.R., Zhang, J.F.J., 2004. Using air pollution based community clusters to explore air pollution health effects in children. *Environment International* 30, 611–620.

Salvador, P., Artinano, B., Alonso, D.G., Querol, X., Alastuey, A., 2004. Identification and characterisation of sources of PM_{10} in Madrid (Spain) by statistical methods. *Atmospheric Environment* 38, 435–447.

Seibert, P., Kromp–Kolb, H., Baltensperger, U., Jost, D.T., Schwikowski, M., Ksaper, A., Puxbaum, H., 1994. Trajectory analysis of aerosol measurements at high Alpine sites, in *Transport and Transformation of Pollutants in the Troposphere*, edited by Borrell, P.M., Borrell, P., Cvitas, T., Seiler, W., Academic Publishing, Den Haag, pp. 689–693.

Sirois, A., Bottenheim, J.W., 1995. Use of backward trajectories to interpret the five–year record of PAN and O_3 ambient air concentrations at Kejimkujik National Park, Nova Scotia. *Journal of Geophysical Research–Atmospheres* 100, 2867–2881.

Stohl, A., 1996. Trajectory statistics – a new method to establish source–receptor relationships of air pollutants and its application to the transport of particulate sulfate in Europe. *Atmospheric Environment* 30, 579–587.

Stohl, A., Kromp-Kolb, H., 1994. Origin of ozone in Vienna and surroundings, Austria. *Atmospheric Environment* 28, 1255–1266.

Wang, G., Ostoja–Starzewski, M., 2004. A numerical study of plume dispersion motivated by a mesoscale atmospheric flow over a complex terrain. *Applied Mathematical Modelling* 28, 957–981.

Wang, F., Chen, D.S., Cheng, S.Y., Li, J.B., Li, M.J., Ren, Z.H., 2010. Identification of regional atmospheric PM_{10} transport pathways using HYSPLIT, MM5–CMAQ and synoptic pressure pattern analysis. *Environmental Modelling & Software* 25, 927–934.

Wang, S.G., Feng, X.Y., Zeng, X.Q., Ma, Y.X., Shang, K.Z., 2009. A study on variations of concentrations of particulate matter with different sizes in Lanzhou, China. *Atmospheric Environment* 43, 2823–2828.

Wang, S.G., Yuan, W., Shang, K.Z., 2006. The impacts of different kinds of dust events on PM_{10} pollution in northern China. *Atmospheric Environment* 40, 7975–7982.

Yu, Y., Xia, D.S., Chen, L.H., Liu, N., Chen, J.B., Gao, Y.H., 2010. Analysis of particulate pollution characteristics and its causes in Lanzhou, Northwest China. *Environmental Science* 31, 22–28.

Zeng, Y., Hopke, P.K., 1989. A study of the sources of acid precipitation in Ontario, Canada. *Atmospheric Environment* 23, 1499–1509.

Zhang, N., Li, L.P., Dong, J.Y., Yuan, Y., Li, L., 2010. Comparative study of water–soluble ions in atmospheric aerosols in Lanzhou in winters of 1990 and 2007. *Research of Environmental Sciences* 23, 647–652.

Zhang, J.F., Hu, W., Wei, F.S., Wu, G.P., Cheng, W.L., Chapman, R.S, 2005. Long–term changes in air pollution and health implications in four Chinese cities. *Energy for Sustainable Development* 9, 67–76.

Zhang, L., Chen, C.H., Murlis, J., 2001. Study on winter air pollution control in Lanzhou, China. *Water, Air & Soil Pollution* 127, 351–372.